

# Natural-Abundance Two-Dimensional $^{29}\text{Si}$ MAS NMR Investigation of the Three-Dimensional Bonding Connectivities in the Zeolite Catalyst ZSM-5

C. A. Fyfe,\* H. Grondey, Y. Feng, and G. T. Kokotailo

Contribution from the Department of Chemistry, University of British Columbia, Vancouver, B.C. V6T 1Y6, Canada. Received May 16, 1990

**Abstract:** Two-Dimensional  $^{29}\text{Si}$  solid-state NMR experiments have been used to investigate the three-dimensional bonding connectivities in zeolite ZSM-5 and also the changes that are induced in the structure by increasing the temperature and by the presence of sorbed *p*-xylene. 2D INADEQUATE experiments gave substantially better results than 2D COSY experiments on the same samples. In the case of the orthorhombic form (12 T-sites) which is formed by increasing the temperature or at a loading of 2 sorbed molecules of *p*-xylene per unit cell, almost all of the expected connectivities were observed. For the monoclinic form, 38 of the total of 48 connectivities were clearly observed, allowing the assignment of the spectrum. When the number of sorbed *p*-xylene molecules is increased above 5 molecules per unit cell, a phase transition from the orthorhombic form with 12 T-sites to another orthorhombic form with 24 T-sites occurs. Due to symmetry, for each of these structures, two possible assignments exist which are compatible with the connectivity pattern. In each case the 2D INADEQUATE experiments yielded sufficient information to determine these two possible assignments. However, without an unambiguous starting point the decision in favor of one assignment against the other cannot be made on the basis of the NMR data alone. Correlating the  $^{29}\text{Si}$  chemical shifts with geometric parameters from X-ray diffraction experiments, however, makes it possible to discriminate in favor of one set of assignments for the orthorhombic (12 T-sites) and yields unambiguous solutions for the monoclinic and the orthorhombic (24 T-sites) forms.

## Introduction

Zeolites are porous aluminosilicate framework structures constructed of linked  $\text{SiO}_4$  and  $\text{AlO}_4$  tetrahedra which are widely used as sorbents and catalysts, the dimensions of the pores and interconnecting channels giving them a unique size and shape selectivity in their interactions with sorbed organic guest molecules.<sup>1,2</sup> Although they are highly crystalline materials, the small size of the crystals (usually of the order of a few microns) precludes the direct application of routine single-crystal diffraction techniques.<sup>3</sup> Thus, structural investigations of these materials usually have to be carried out with use of much more limited powder diffraction techniques combined with information from other sources.<sup>4</sup>

In this regard, high-resolution solid-state NMR spectroscopy has emerged as a complementary technique to the traditional diffraction methods, probing local geometries and short-range orderings in contrast to the much longer range periodicities that form the basis for diffraction studies.<sup>5</sup> In the case of low Si/Al ratio materials, five resonances are observed in the simplest cases, corresponding to the five possible local silicon environments Si-[4Al], Si[3Al,1Si], ..., Si[4Si] that describe the average Si, Al distributions throughout the framework,<sup>6</sup> information that is not obtainable from the (average) X-ray structures. In the case of highly siliceous zeolites, there is an even more direct relationship between the  $^{29}\text{Si}$  spectra and the lattice structure: The removal of Al generates a perfectly ordered system as all of the silicons have the same local environment Si[4Si]. This results in the  $^{29}\text{Si}$  resonances being very narrow, and a series of signals are observed for structures with more than one crystallographically inequivalent site, the numbers and relative intensities of which reflect directly the numbers and occupancies of the T-sites in the asymmetric unit of the unit cell.<sup>7</sup> Previous work in our group has centered on the optimization of these spectra which are often much more sensitive than diffraction data to local orderings and also their use together with synchrotron-based powder X-ray diffraction measurements to determine exact structures and the effects of temperature and sorbed organic molecules on the structures.<sup>8</sup>

In an attempt to further develop the interactive relationship between the NMR and XRD techniques, we have recently investigated the possibility of obtaining the three-dimensional

Table I. Description of the Sample Investigated in the Present Work

| Sample                             | Sample and Conditions                                   | Space Group (ref.)                              | T-sites in the asymmetric unit | Name given in following discussion |
|------------------------------------|---|---|--------------------------------|------------------------------------|
| ZSM-5                              | ambient temperature (300K)                              | monoclinic form<br>$P2_1/n$<br>(21)             | 24                             | Monoclinic phase                   |
|                                    | high temperature (403K)                                 | orthorhombic form<br>$Pnma$ (22)<br>$Pnma$ (23) | 12                             | Orthorhombic phase (12 T-sites)    |
| ZSM-5 with sorbed <i>p</i> -xylene | low-loading with <i>p</i> -xylene (2 molecules/UC) 300K |   |                                |                                    |
|                                    | high-loaded (8 molecules/UC) 293K                       | orthorhombic form $P2_12_12_1$ (28)             | 24                             | Orthorhombic phase (24 T-sites)    |

bonding connectivities in these structures from two-dimensional NMR experiments. In initial studies on enriched materials

(1) (a) Barrer, R. M. *Zeolites and Clay Minerals*; Academic Press: London, 1978. (b) Rabo, J. A. *Zeolite Chemistry and Catalysis*; ACS Monograph 171; American Chemical Society: Washington DC, 1976. (c) Breck, D. W. *Zeolite Molecular Sieves*; Wiley: New York, 1974.

(2) Meier, W. M.; Olson, D. H. *Atlas of Zeolites Structure Types*; Structure Commission of the International Zeolite Association, 1978.

(3) It has recently been demonstrated that the use of synchrotron X-ray sources permits single-crystal studies to be carried out on much smaller samples. Eisenberger, P.; Newsam, J. B.; Leonowicz, M. E.; Vaughan, D. E. W. *Nature (London)* **1984**, *45*, 309.

(4) The use of Rietveld refinement techniques allows better structural information to be obtained from powder diffraction data. David, W. I. F.; Harrison, W. T. A.; Johnson, M. W. *High Resolution Powder Diffraction*; Materials Science Forum; Catlow, C.R.A., Ed.; Trans. Tech. Publication: Andernansdorf, Switzerland; Vol. 9, pp 89-101.

(5) Engelhardt, G.; Michel, D. *High-Resolution Solid State NMR of Silicates and Zeolites*; John Wiley and Sons: New York, 1987.

(6) (a) Lippmaa, E.; Magi, M.; Samoson, A.; Tarmak, M.; Engelhardt, G. *J. Am. Chem. Soc.* **1981**, *103*, 4992. (b) Lippmaa, E.; Magi, M.; Samoson, A.; Engelhardt, G.; Grimmer, A. R. *J. Am. Chem. Soc.* **1980**, *102*, 4889.

\* Author to whom enquires should be addressed.

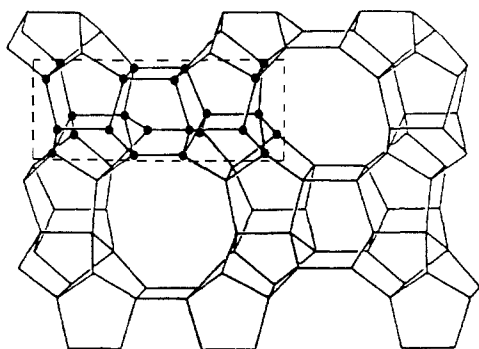


**Figure 1.** Skeletal diagram of the (100)-face of the ZSM-5 unit cell (oxygen atoms are not shown). The asymmetric unit is indicated by the 24 T-sites with solid circles.

known structures we demonstrated that COSY and spin-diffusion experiments yielded the correct (known) connectivities for zeolite ZSM-39<sup>9</sup> and that COSY and INADEQUATE experiments were similarly in agreement with the expected connectivities for zeolite DD3R.<sup>10</sup> The results of these experiments laid the groundwork for subsequent studies with only the 4.7% natural abundance of <sup>29</sup>Si, and we have recently demonstrated the viability of such connectivity experiments for the two representative zeolites ZSM-12 and ZSM-22.<sup>11</sup> Particularly importantly, the scalar <sup>29</sup>Si/<sup>29</sup>Si spin-spin couplings were observed directly in these studies and their numerical values could be used to implement further experiments. Thus, the INADEQUATE sequence could be carried out very efficiently, giving improved S/N and no interferences from signals originating from the majority of <sup>29</sup>Si nuclei which are not part of <sup>29</sup>Si-O-<sup>29</sup>Si bonding pairs.

In the present work, we present the results of the application of these techniques to the most complex zeolite structure known, in terms of the large asymmetric unit in its unit cell, zeolite ZSM-5, both in its low-temperature monoclinic phase and the orthorhombic phases to which it is converted by the action of temperature and/or *p*-xylene. A summary of the different phases investigated in this study is given in Table I.

### Experimental Section

Highly siliceous zeolite ZSM-5 was synthesized hydrothermally according to literature techniques but with added ammonium bifluoride for 5 days at 170 °C. The template used was tetrapropylammonium ion. The isolated, washed, and calcined material was dealuminated one or more times with water vapor for 9 days at 800 °C to produce completely siliceous, fault and defect free material.<sup>12</sup>

The loaded *p*-xylene samples were prepared by activating highly siliceous zeolite ZSM-5 at 500 °C for 4 h. After the sample was cooled to room temperature various amounts of *p*-xylene were added to weighed amounts of ZSM-5. The samples were cooled to liquid nitrogen temperature and then fire-sealed under vacuum. They were then kept in an oven at 100 °C for periods up to several days to ensure an equilibrium distribution of the sorbate.

<sup>29</sup>Si MAS NMR spectra were obtained at 79.5 MHz on a Bruker MSL-400 spectrometer with the "magic angle" accurately set with use of the <sup>79</sup>Br resonance of KBr.<sup>13</sup> 2D experiments were carried out with

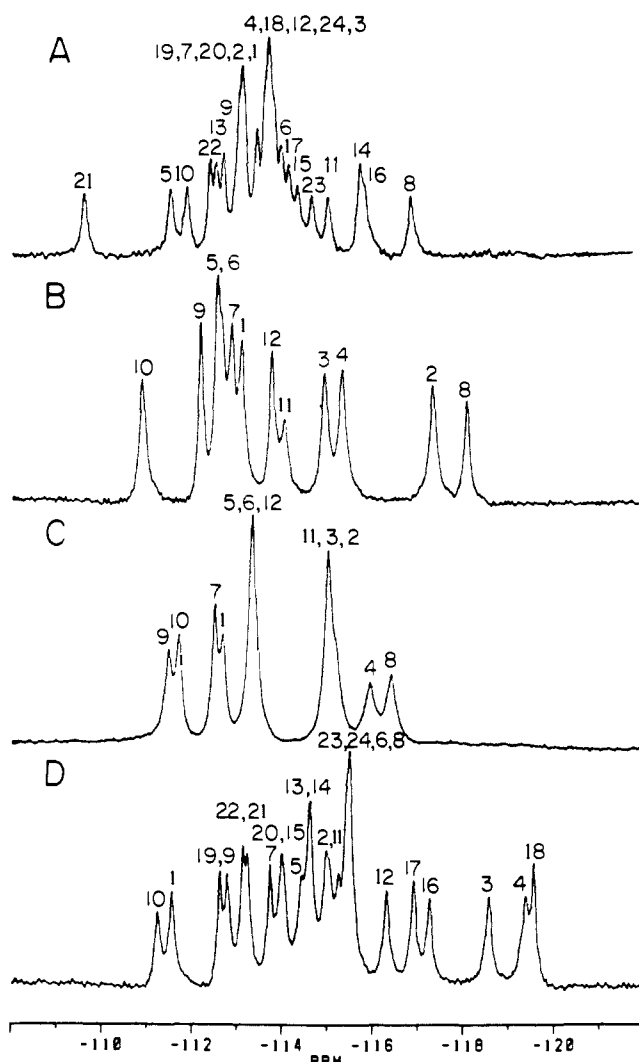


**Figure 2.** (A) <sup>29</sup>Si MAS NMR spectrum of ZSM-5 at 300 K. (B) <sup>29</sup>Si MAS NMR spectrum of low-loaded ZSM-5 (2 molecules of *p*-xylene per 96 T-atom unit cell) at 300 K. (C) <sup>29</sup>Si MAS NMR spectrum of ZSM-5 at 403 K. (D) <sup>29</sup>Si CP/MAS NMR spectrum of high-loaded ZSM-5 (8 molecules of *p*-xylene per 96 T-atom unit cell) at 293 K. The assignments of the individual resonances of the four spectra are indicated.

a commercial pulse-programmer and software. In the case of the high-loaded form of ZSM-5/*p*-xylene, <sup>1</sup>H/<sup>29</sup>Si cross-polarization was efficient and the initial 90° pulse of the INADEQUATE experiment was replaced by a CP sequence.<sup>14</sup> Complete details of the experimental parameters used for each experiment are given in the appropriate figure captions. <sup>29</sup>Si chemical shifts are indexed wrt. TMS taking the highest resonance line of Q<sub>8</sub>M<sub>8</sub> to be -109.7 ppm.

### Results and Discussion

Zeolite ZSM-5 is the prototype of a family of zeolites based on the pentasil structural unit. Its structure is shown in Figure 1 with the T-sites in the asymmetric unit indicated by the filled circles. The original structure refinement,<sup>15a</sup> which described the unit cell as orthorhombic, space group *Pnma*, has been followed by a number of investigations<sup>15b-23</sup> including a single-crystal study

(7) (a) Fyfe, C. A.; Gobbi, G. C.; Murphy, W. J.; Ozubko, R. S.; Slack, D. A. *Chem. Lett.* **1983**, 1547. (b) Fyfe, C. A.; Gobbi, G. C.; Murphy, W. J.; Ozubko, R. S.; Slack, D. A. *J. Am. Chem. Soc.* **1984**, *106*, 4435. (c) Klinowski, J.; Thomas, J. M.; Audier, M.; Vasudevan, S.; Fyfe, C. A.; Hartman, J. S. *J. Chem. Soc., Chem. Commun.* **1981**, 570. (d) Fyfe, C. A.; Gobbi, G. C.; Kennedy, G. J.; DeSchutter, C. T. *Chem. Lett.* **1984**, 2, 163. (e) Thomas, J. M.; Klinowski, J.; Ramdas, S.; Hunter, B. K.; Tennakoon, E. D. *J. Am. Chem. Soc.* **1983**, *105*, 158.

(8) Fyfe, C. A.; Gies, H.; Kokotailo, G. T.; Feng, Y.; Strobl, H. J.; Marler, B.; Cox, D. E. *Zeolites: Facts, Figures, Future*; Jacobs, P. A., van Santen, R. A., Eds.; Elsevier Science Publishers: Amsterdam, 1989.

(9) (a) Fyfe, C. A.; Gies, H.; Feng, Y. *Chem. Commun.* **1989**, 1240. (b) Fyfe, C. A.; Gies, H.; Feng, Y. *J. Am. Chem. Soc.* **1989**, *111*, 7702.

(10) Fyfe, C. A.; Gies, H.; Feng, Y.; Grondey, H. *Zeolites*. In press.

(11) (a) Fyfe, C. A.; Feng, Y.; Gies, H.; Kokotailo, G. T. *Nature* **1989**, *341*, 6239. (b) Fyfe, C. A.; Feng, Y.; Gies, H.; Grondey, H.; Kokotailo, G. T. *J. Am. Chem. Soc.* In press.

(12) Fyfe, C. A.; Strobl, H. J.; Kokotailo, G. T.; Kennedy, G. J.; Barlow, G. E. *J. Am. Chem. Soc.* **1988**, *110*, 3373.

(13) Frye, J. S.; Maciel, G. E. *J. Magn. Reson.* **1982**, *48*, 125.

(14) (a) Benn, R.; Grondey, H.; Brevard, C.; Pagelot, A. *J. Chem. Soc., Chem. Commun.* **1988**, 102. (b) Early, T. A.; John, B. K. I.; Johnson, L. F. *J. Magn. Reson.* **1987**, *75*, 134.

(15) (a) Kokotailo, G. T.; Lawton, S. L.; Olson, D. H.; Meier, W. M. *Nature (London)* **1978**, *272*, 437. (b) Olson, D. H.; Kokotailo, G. T.; Lawton, S. L.; Meier, W. M. *J. Phys. Chem.* **1981**, *85*, 2238-2243.

(16) Lermer, H.; Draeger, M.; Steffen, J.; Unger, K. K. *Zeolites* **1985**, *5*, 13.

(17) Chao, K.; Lin, J.; Wang, Y.; Lee, G. H. *Zeolites* **1985**, *6*, 35.

(18) Baerlocher, C. *Proceedings of the 6th International Conference on Zeolites, Reno, 1983*; Butterworths: London, 1984.

(19) (a) Price, G. D.; Pluth, J. J.; Smith, J. V.; Bennett, J. M.; Patton, R. L. *J. Am. Chem. Soc.* **1982**, *104*, 5971. (b) van Koningsveld, H.; van Bekkum, H.; Jansen, J. E. *Acta Crystallogr.* **1987**, *B43*, 127.

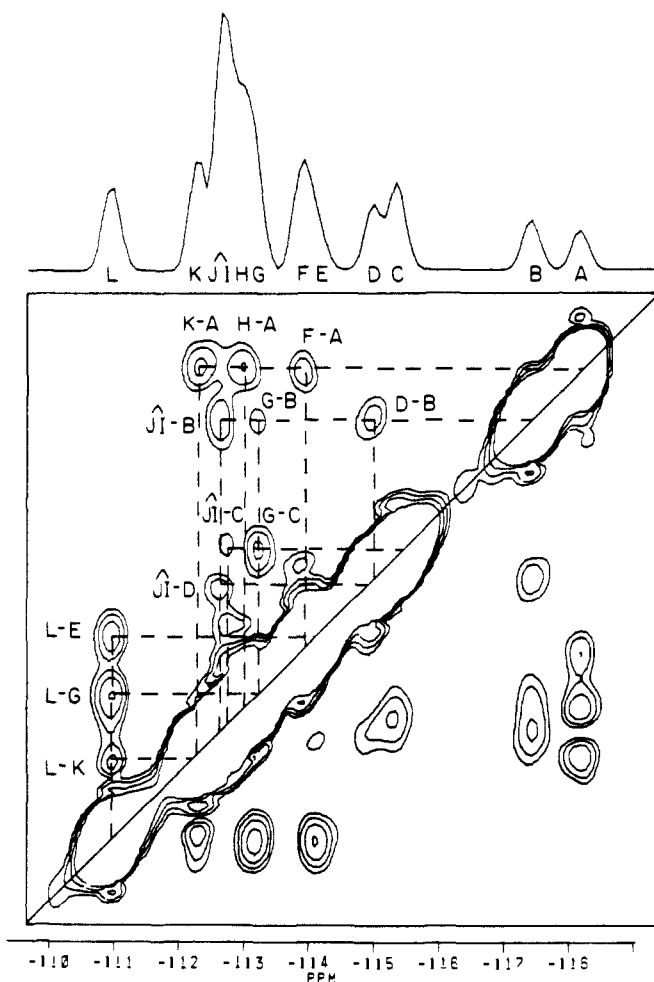


**Figure 3.** Contour plot of a COSY 45 experiment on ZSM-5 with 2 molecules of *p*-xylene per unit cell with the projection in the F2 dimension shown on top. The temperature was 300 K, and 64 experiments were carried out with 576 scans in each experiment. A sweep width of 1700 Hz, a fixed delay of 10 ms, and 220 real data points were used. Sine-bell-squared apodization and power calculation were used for the data processing.

of the location of the template in the as-synthesized material<sup>19</sup> and recent single-crystal<sup>21</sup> and synchrotron X-ray powder studies of highly siliceous samples at both low and high temperatures.<sup>18,22</sup>

High-resolution <sup>29</sup>Si MAS NMR investigations have demonstrated that the room temperature form of the completely siliceous material is monoclinic with 24 T-sites and that a structural change to an orthorhombic form with 12 T-sites is induced by increasing the temperature or by the addition of 2 molecules of *p*-xylene per unit cell.<sup>8,12,24</sup> In the latter case, the change is gradual, both forms being crystalline and co-existing at intermediate conversions while for the thermally induced change the monoclinic 24 to orthorhombic 12 T-site turnover occurs over a very small temperature range. Figure 2 shows the one-dimensional <sup>29</sup>Si MAS NMR spectra of the four systems that were investigated in the present study obtained under similar conditions to those used for the 2D experiments. The numbering of the different resonances in each spectrum comes from the 2D-NMR spectroscopy of the present work (see latter). The substantial changes observed in the peak

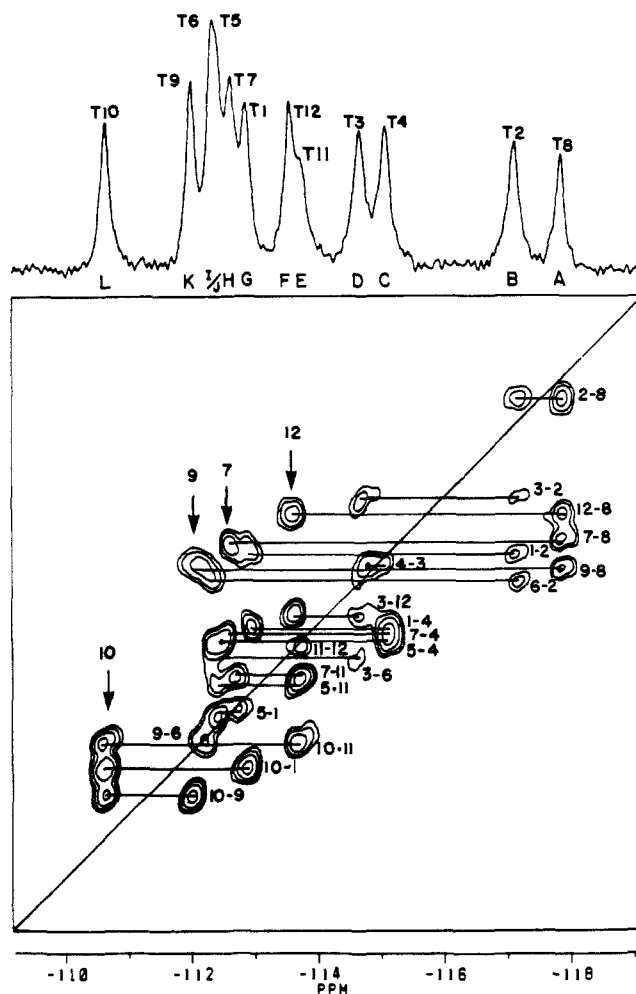


**Figure 4.** Contour plot of an INADEQUATE experiment on ZSM-5 with 2 molecules of *p*-xylene per unit cell carried out at 300 K with a 1D MAS NMR spectrum above. 36 experiments with 512 scans in each experiment were performed with a recycle time of 14 s, and the total time for the experiment was approximately 72 h. A sweep width of 800 Hz, a fixed delay of 15 ms, and 140 real data points were used. Sine-bell and trapezoidal apodizations in the F2 and F1 dimensions respectively and a power calculation were used for the data processing.

positions reflect clearly the changes in local T-site geometries induced in the structure by these transformations.

The ZSM-5 structure is a particularly difficult one to investigate by 2D-NMR connectivity experiments and represents the most demanding test possible of these techniques at the present time: First, the structure itself is very complex, the asymmetric unit containing either 24 or 12 T-sites, and a very large number of <sup>29</sup>Si-O-<sup>29</sup>Si connectivities will occur within the 2D plots. Second, there is no readily available starting point, in terms of an unambiguously assignable resonance, which can be used to begin working through the connectivity patterns. All of the T-sites have equal occupancies, precluding the assignment of any of the resonances on the basis of their relative intensities. In addition, as can be seen from Figure 1, all of the T-sites occupy positions on the walls of the channels, exposing them to sorbed molecular oxygen which provides the primary relaxation mechanism for the <sup>29</sup>Si nuclei. Thus all of the nuclei have relatively short and quite similar spin-lattice relaxation times, eliminating this parameter as a way of assigning any individual resonances as was done previously for zeolites ZSM-12 and ZSM-22.<sup>11</sup> However, in the present work, the investigations are of different phases of the same system and it may be possible to trace the gradual changes of the resonances in the 1D <sup>29</sup>Si MAS NMR spectra induced by raising temperature and/or sorbed *p*-xylene as previously described<sup>12</sup> and thus relate the resonances in some of the spectra to each other. In this way the assignments of the different 2D spectra may be checked for self-consistency.

(20) Wu, E. L.; Lawton, S. L.; Olson, D. H.; Rohrman, A. C.; Kokotailo, G. T. *J. Phys. Chem.* **1979**, *83*, 2777.

(21) van Koningsveld, H.; Jansen, J. C.; van Bekkum, H. *Zeolites* **1990**, *10*, 235.

(22) Gies, H., and co-workers, to be published.

(23) Gies, H.; Marler, B.; and co-workers, unpublished work.

(24) (a) Fyfe, C. A.; Kennedy, G. J.; DeSchutter, C. T.; Kokotailo, G. T. *J. Chem. Soc., Chem. Commun.* **1984**, 541. (b) West, G. W. *Aust. J. Chem.* **1984**, *37*, 455. (c) Fyfe, C. A.; Kokotailo, G. T.; Lyster, J. R.; Flemming, W. W. *J. Chem. Soc., Chem. Commun.* **1985**, 740. (d) Hay, D. G.; Jaeger, H.; West, G. W. *J. Phys. Chem.* **1985**, *89*, 1070.

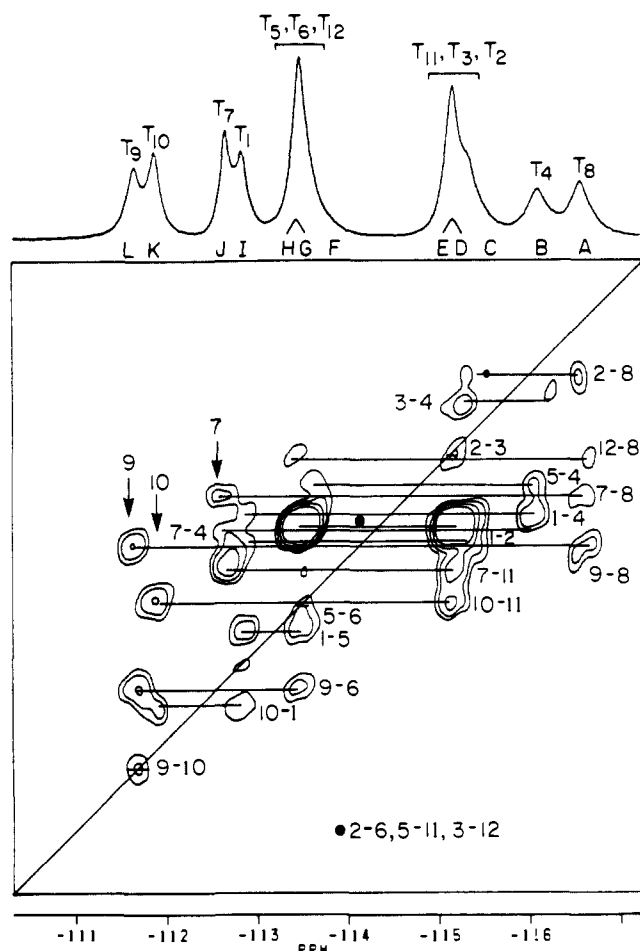


**Figure 5.** Contour plot of an INADEQUATE experiment on ZSM-5 at 403 K with a 1D MAS NMR spectrum above. 32 experiments with 352 scans in each experiment were carried out with the recycle time of 50 s, and the total time for the experiment was approximately 157 h. A sweep width of 550 Hz, a fixed delay of 15 ms, and 108 real data points were used. Sine-bell and trapezoidal apodizations in the F2 and F1 dimensions respectively and a power calculation were used for the data processing.

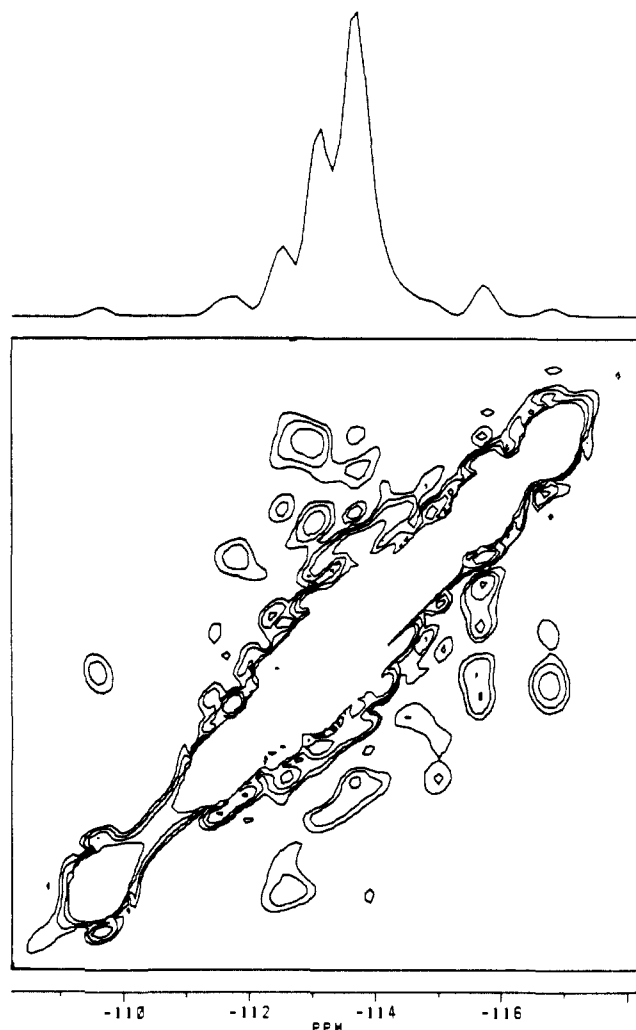
The structural elements and the expected connectivities for the three phases are presented in Tables II–IV together with their asymmetric structural units. In order to facilitate the discussion of the connectivities, the resonance lines have been arbitrarily designated A, B, C, ..., X from highest to lowest field as indicated in Figures 3, 4, 5, 7, and 9. When individual resonances have been assigned, they have been labeled 1, 2, ... with the numbering corresponding to the indexing of the T-sites shown in Tables II–IV. It should be noted that the 1D spectra were obtained with parameters corresponding to those of the 2D experiments and thus the resolution reflects that of the 2D data.

**I. Orthorhombic Structures (12 T-Sites).** Since the orthorhombic form is the more symmetrical structure, it was investigated first. The phase transition from monoclinic to orthorhombic symmetry can be induced either by raising the temperature or by adsorbing *p*-xylene or by a combination of both. In agreement with Rietveld refined X-ray diffraction data the NMR spectra indicate that no matter how the phase transition is accomplished, the same lattice symmetry results and therefore the same connectivity pattern.

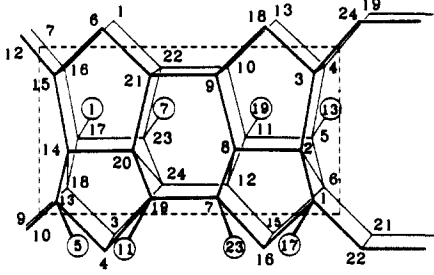
However, local geometric parameters, for example the T–T distances, which depend on the temperature and on the sorbate, have a strong influence on the  $^{29}\text{Si}$  chemical shifts. Thus the NMR spectrum of pure ZSM-5 at 403 K and the one of ZSM-5 loaded with 2 molecules of *p*-xylene per unit cell are quite distinct (cf. Figure 2B,C). Although it is possible to trace some lines through a series of spectra at 400 K from samples containing various amounts of *p*-xylene and variable-temperature experiments on a sample with 2 molecules of *p*-xylene per unit cell, an unambiguous

**Table II.** T-Sites, Their Occupancies, and Connectivities for the Asymmetric Unit in the Orthorhombic Phase (12 T-Sites) of ZSM-5

| T-site          | occupancy | connectivities   |
|-----------------|-----------|--|
| T <sub>1</sub>  | 1         | 1T <sub>2</sub> :1T <sub>4</sub> :1T <sub>10</sub> :1T <sub>5</sub>  |
| T <sub>2</sub>  | 1         | 1T <sub>1</sub> :1T <sub>3</sub> :1T <sub>6</sub> :1T <sub>8</sub>   |
| T <sub>3</sub>  | 1         | 1T <sub>2</sub> :1T <sub>4</sub> :1T <sub>6</sub> :1T <sub>12</sub>  |
| T <sub>4</sub>  | 1         | 1T <sub>3</sub> :1T <sub>5</sub> :1T <sub>7</sub> :1T <sub>11</sub>  |
| T <sub>5</sub>  | 1         | 1T <sub>4</sub> :1T <sub>6</sub> :1T <sub>11</sub> :1T <sub>1</sub>  |
| T <sub>6</sub>  | 1         | 1T <sub>2</sub> :1T <sub>5</sub> :1T <sub>3</sub> :1T <sub>9</sub>   |
| T <sub>7</sub>  | 1         | 1T <sub>8</sub> :1T <sub>7</sub> :1T <sub>4</sub> :1T <sub>11</sub>  |
| T <sub>8</sub>  | 1         | 1T <sub>2</sub> :1T <sub>7</sub> :1T <sub>9</sub> :1T <sub>12</sub>  |
| T <sub>9</sub>  | 1         | 1T <sub>8</sub> :1T <sub>10</sub> :1T <sub>9</sub> :1T <sub>6</sub>  |
| T <sub>10</sub> | 1         | 1T <sub>6</sub> :1T <sub>11</sub> :1T <sub>10</sub> :1T <sub>1</sub> |
| T <sub>11</sub> | 1         | 1T <sub>5</sub> :1T <sub>10</sub> :1T <sub>12</sub> :1T <sub>7</sub> |
| T <sub>12</sub> | 1         | 1T <sub>8</sub> :1T <sub>12</sub> :1T <sub>11</sub> :1T <sub>3</sub> |



**Figure 6.** Contour plot of a COSY 45 experiment on ZSM-5 at 293 K with the projection on F2 shown above. 64 experiments with 816 scans in each experiment were carried out with a recycle time of 8 s, and the total time for the experiment was approximately 116 h. A sweep width of 2000 Hz, a fixed delay of 10 ms, and 180 real data points were used. Sine-bell apodization in the F1 and F2 and a power calculation were used for the data processing.

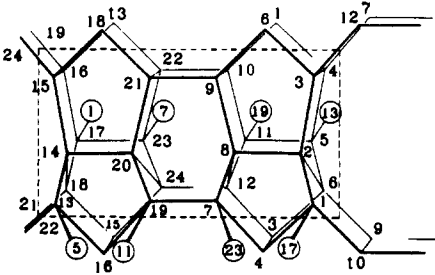
**Table III.** T-Sites, Their Occupancies, and Connectivities for the Asymmetric Unit in the Monoclinic Phase of ZSM-5


| T-site          | occupancy | connectivities   |
|-----------------|-----------|--|
| T <sub>1</sub>  | 1         | 1T <sub>2</sub> :1T <sub>16</sub> :1T <sub>17</sub> :1T <sub>22</sub>  |
| T <sub>2</sub>  | 1         | 1T <sub>1</sub> :1T <sub>3</sub> :1T <sub>6</sub> :1T <sub>8</sub>     |
| T <sub>3</sub>  | 1         | 1T <sub>2</sub> :1T <sub>4</sub> :1T <sub>18</sub> :1T <sub>24</sub>   |
| T <sub>4</sub>  | 1         | 1T <sub>3</sub> :1T <sub>5</sub> :1T <sub>13</sub> :1T <sub>19</sub>   |
| T <sub>5</sub>  | 1         | 1T <sub>4</sub> :1T <sub>6</sub> :1T <sub>11</sub> :1T <sub>13</sub>   |
| T <sub>6</sub>  | 1         | 1T <sub>2</sub> :1T <sub>5</sub> :1T <sub>15</sub> :1T <sub>21</sub>   |
| T <sub>7</sub>  | 1         | 1T <sub>8</sub> :1T <sub>16</sub> :1T <sub>19</sub> :1T <sub>23</sub>  |
| T <sub>8</sub>  | 1         | 1T <sub>2</sub> :1T <sub>7</sub> :1T <sub>9</sub> :1T <sub>12</sub>    |
| T <sub>9</sub>  | 1         | 1T <sub>8</sub> :1T <sub>10</sub> :1T <sub>18</sub> :1T <sub>21</sub>  |
| T <sub>10</sub> | 1         | 1T <sub>6</sub> :1T <sub>11</sub> :1T <sub>13</sub> :1T <sub>22</sub>  |
| T <sub>11</sub> | 1         | 1T <sub>5</sub> :1T <sub>10</sub> :1T <sub>12</sub> :1T <sub>19</sub>  |
| T <sub>12</sub> | 1         | 1T <sub>8</sub> :1T <sub>11</sub> :1T <sub>15</sub> :1T <sub>24</sub>  |
| T <sub>13</sub> | 1         | 1T <sub>4</sub> :1T <sub>5</sub> :1T <sub>10</sub> :1T <sub>14</sub>   |
| T <sub>14</sub> | 1         | 1T <sub>13</sub> :1T <sub>15</sub> :1T <sub>18</sub> :1T <sub>20</sub> |
| T <sub>15</sub> | 1         | 1T <sub>6</sub> :1T <sub>12</sub> :1T <sub>14</sub> :1T <sub>16</sub>  |
| T <sub>16</sub> | 1         | 1T <sub>1</sub> :1T <sub>7</sub> :1T <sub>15</sub> :1T <sub>17</sub>   |
| T <sub>17</sub> | 1         | 1T <sub>1</sub> :1T <sub>16</sub> :1T <sub>18</sub> :1T <sub>23</sub>  |
| T <sub>18</sub> | 1         | 1T <sub>3</sub> :1T <sub>9</sub> :1T <sub>14</sub> :1T <sub>17</sub>   |
| T <sub>19</sub> | 1         | 1T <sub>4</sub> :1T <sub>7</sub> :1T <sub>11</sub> :1T <sub>20</sub>   |
| T <sub>20</sub> | 1         | 1T <sub>14</sub> :1T <sub>19</sub> :1T <sub>21</sub> :1T <sub>24</sub> |
| T <sub>21</sub> | 1         | 1T <sub>6</sub> :1T <sub>9</sub> :1T <sub>20</sub> :1T <sub>22</sub>   |
| T <sub>22</sub> | 1         | 1T <sub>1</sub> :1T <sub>10</sub> :1T <sub>21</sub> :1T <sub>23</sub>  |
| T <sub>23</sub> | 1         | 1T <sub>7</sub> :1T <sub>17</sub> :1T <sub>22</sub> :1T <sub>24</sub>  |
| T <sub>24</sub> | 1         | 1T <sub>3</sub> :1T <sub>12</sub> :1T <sub>20</sub> :1T <sub>23</sub>  |

correlation between all of the peaks in the two spectra cannot be established from the 1D spectra alone due to peak crossing and/or overlap, and both species were investigated in detail by 2D homonuclear correlation experiments.

A series of <sup>29</sup>Si 2D COSY experiments were carried out on the *p*-xylene loaded form (2 molecules per unit cell) with use of the simple [90<sub>x</sub>-t<sub>1</sub>-FD-45<sub>x</sub>-FD-t<sub>2</sub>(acquisition)] sequence with the fixed delay (FD) adjusted to optimize the connectivities.<sup>25</sup> The results from a typical experiment are shown in Figure 3 without symmetrization. There are clear indications of a number of connectivities between different silicons, 12 of the expected 22 being clearly observed as indicated in the figure, but there is not enough information available from this experiment to assign individual resonances. In part, this is due to there being no unique signals in terms of either relative intensities or spin-lattice relaxation times with which to begin assignments as discussed above. However, in addition, the very large intensities that occur along the diagonal obscure those cross-peaks close to the diagonal, limiting the number that can be observed and subsequently used in the spectral assignment. From Figures 2B and 3, it can be seen that a majority of the signals are grouped together near the center of the spectrum, and it must be anticipated that a substantial number of connectivities between signals of similar resonance frequencies will be obscured in simple COSY experiments. This problem will be even worse for the monoclinic form (Figure 2A).

In an attempt to solve this problem, <sup>29</sup>Si 2D experiments using an INADEQUATE sequence were carried out.<sup>26</sup> The pulse sequence used was the conventional [90<sub>x</sub>-FD-180<sub>x</sub>-FD-90<sub>x</sub>-t<sub>1</sub>-135<sub>x</sub>-t<sub>2</sub>(acquisition)] one,<sup>26a</sup> yielding a 2D plot where only double quantum coherence signals are observed, that is only signals

**Table IV.** T-Sites, Their Occupancies, and Connectivities for the Asymmetric Unit in the Orthorhombic Phase (24 T-Sites) of ZSM-5


| T-site          | occupancy | connectivities   |
|-----------------|-----------|--|
| T <sub>1</sub>  | 1         | 1T <sub>2</sub> :1T <sub>4</sub> :1T <sub>10</sub> :1T <sub>17</sub>   |
| T <sub>2</sub>  | 1         | 1T <sub>1</sub> :1T <sub>3</sub> :1T <sub>6</sub> :1T <sub>8</sub>     |
| T <sub>3</sub>  | 1         | 1T <sub>2</sub> :1T <sub>4</sub> :1T <sub>6</sub> :1T <sub>12</sub>    |
| T <sub>4</sub>  | 1         | 1T <sub>1</sub> :1T <sub>3</sub> :1T <sub>5</sub> :1T <sub>7</sub>     |
| T <sub>5</sub>  | 1         | 1T <sub>4</sub> :1T <sub>6</sub> :1T <sub>11</sub> :1T <sub>13</sub>   |
| T <sub>6</sub>  | 1         | 1T <sub>2</sub> :1T <sub>5</sub> :1T <sub>3</sub> :1T <sub>9</sub>     |
| T <sub>7</sub>  | 1         | 1T <sub>4</sub> :1T <sub>8</sub> :1T <sub>19</sub> :1T <sub>23</sub>   |
| T <sub>8</sub>  | 1         | 1T <sub>2</sub> :1T <sub>7</sub> :1T <sub>9</sub> :1T <sub>12</sub>    |
| T <sub>9</sub>  | 1         | 1T <sub>6</sub> :1T <sub>8</sub> :1T <sub>10</sub> :1T <sub>21</sub>   |
| T <sub>10</sub> | 1         | 1T <sub>1</sub> :1T <sub>9</sub> :1T <sub>11</sub> :1T <sub>22</sub>   |
| T <sub>11</sub> | 1         | 1T <sub>5</sub> :1T <sub>10</sub> :1T <sub>12</sub> :1T <sub>19</sub>  |
| T <sub>12</sub> | 1         | 1T <sub>3</sub> :1T <sub>11</sub> :1T <sub>6</sub> :1T <sub>24</sub>   |
| T <sub>13</sub> | 1         | 1T <sub>5</sub> :1T <sub>14</sub> :1T <sub>16</sub> :1T <sub>22</sub>  |
| T <sub>14</sub> | 1         | 1T <sub>13</sub> :1T <sub>15</sub> :1T <sub>18</sub> :1T <sub>20</sub> |
| T <sub>15</sub> | 1         | 1T <sub>4</sub> :1T <sub>16</sub> :1T <sub>18</sub> :1T <sub>24</sub>  |
| T <sub>16</sub> | 1         | 1T <sub>13</sub> :1T <sub>15</sub> :1T <sub>17</sub> :1T <sub>19</sub> |
| T <sub>17</sub> | 1         | 1T <sub>1</sub> :1T <sub>16</sub> :1T <sub>18</sub> :1T <sub>23</sub>  |
| T <sub>18</sub> | 1         | 1T <sub>14</sub> :1T <sub>15</sub> :1T <sub>17</sub> :1T <sub>21</sub> |
| T <sub>19</sub> | 1         | 1T <sub>7</sub> :1T <sub>16</sub> :1T <sub>11</sub> :1T <sub>20</sub>  |
| T <sub>20</sub> | 1         | 1T <sub>14</sub> :1T <sub>19</sub> :1T <sub>21</sub> :1T <sub>24</sub> |
| T <sub>21</sub> | 1         | 1T <sub>9</sub> :1T <sub>18</sub> :1T <sub>20</sub> :1T <sub>22</sub>  |
| T <sub>22</sub> | 1         | 1T <sub>10</sub> :1T <sub>13</sub> :1T <sub>21</sub> :1T <sub>23</sub> |
| T <sub>23</sub> | 1         | 1T <sub>7</sub> :1T <sub>17</sub> :1T <sub>22</sub> :1T <sub>24</sub>  |
| T <sub>24</sub> | 1         | 1T <sub>15</sub> :1T <sub>12</sub> :1T <sub>20</sub> :1T <sub>23</sub> |

due to <sup>29</sup>Si nuclei which are coupled. The F<sub>2</sub> domain is the normal chemical shift frequency scale and the F<sub>1</sub> domain represents the double-quantum frequencies of the resonances. Connected signals occur equally spaced on either side of the diagonal of the plot at the same frequencies in F<sub>2</sub> as the corresponding resonances from a simple 1D experiment. In addition to the simplification of the plot from the use of a double-quantum filter, there are a number of other advantages involving better S/N that arise in using the INADEQUATE experiment to establish connectivities. Thus, the intensities of the cross-peaks increase as the coupling in F<sub>1</sub> is eliminated and also an optimum dynamic range can be employed as there are no large single quantum resonances. Further, very efficient apodization functions may be chosen for the data analysis. An additional increase in S/N comes from the fact that all individual experiments in the INADEQUATE 2D sequence contribute substantially to the final intensities. Thus, if the *J* couplings are known (and the experiment is relatively sensitive to this), the fixed delay (FD) may be set at its optimum value of (1/*qJ*) with a corresponding optimization of the intensities observed in the final 2D plot. From our previous natural-abundance <sup>29</sup>Si experiments, the <sup>29</sup>Si-O-<sup>29</sup>Si *J* couplings are known to be in the range of 10–15 Hz,<sup>11</sup> and this range was used to carry out one or several experiments with different FD's that were added together to get various connectivities with different *J* couplings. From these experiments, a FD value of 16 ms seemed optimum, and this was used in subsequent experiments. It was thus anticipated that better S/N should be obtained and more connectivities observed.

Figure 4 shows the results of a 2D INADEQUATE experiment carried out on the same low-loaded material with use of the parameters indicated in the figure caption. As can be seen, many more connectivities are observed, 21 in all, which from Table II means that almost every single possible Si-O-Si bonding interaction has been detected. In complex systems such as the subjects of the present investigation, the INADEQUATE sequence is clearly superior in detecting the bonding connectivities, and this

(25) Muller, L.; Kumar, A.; Ernst, R. R. *J. Chem. Phys.* **1975**, *63*, 5490.(26) (a) Bax, A.; Freeman, R.; Frenkiel, T. A.; Levitt, J. *J. Magn. Reson.* **1981**, *43*, 478. (b) Mareci, T. H.; Freeman, R. *J. Magn. Reson.* **1982**, *48*, 158.

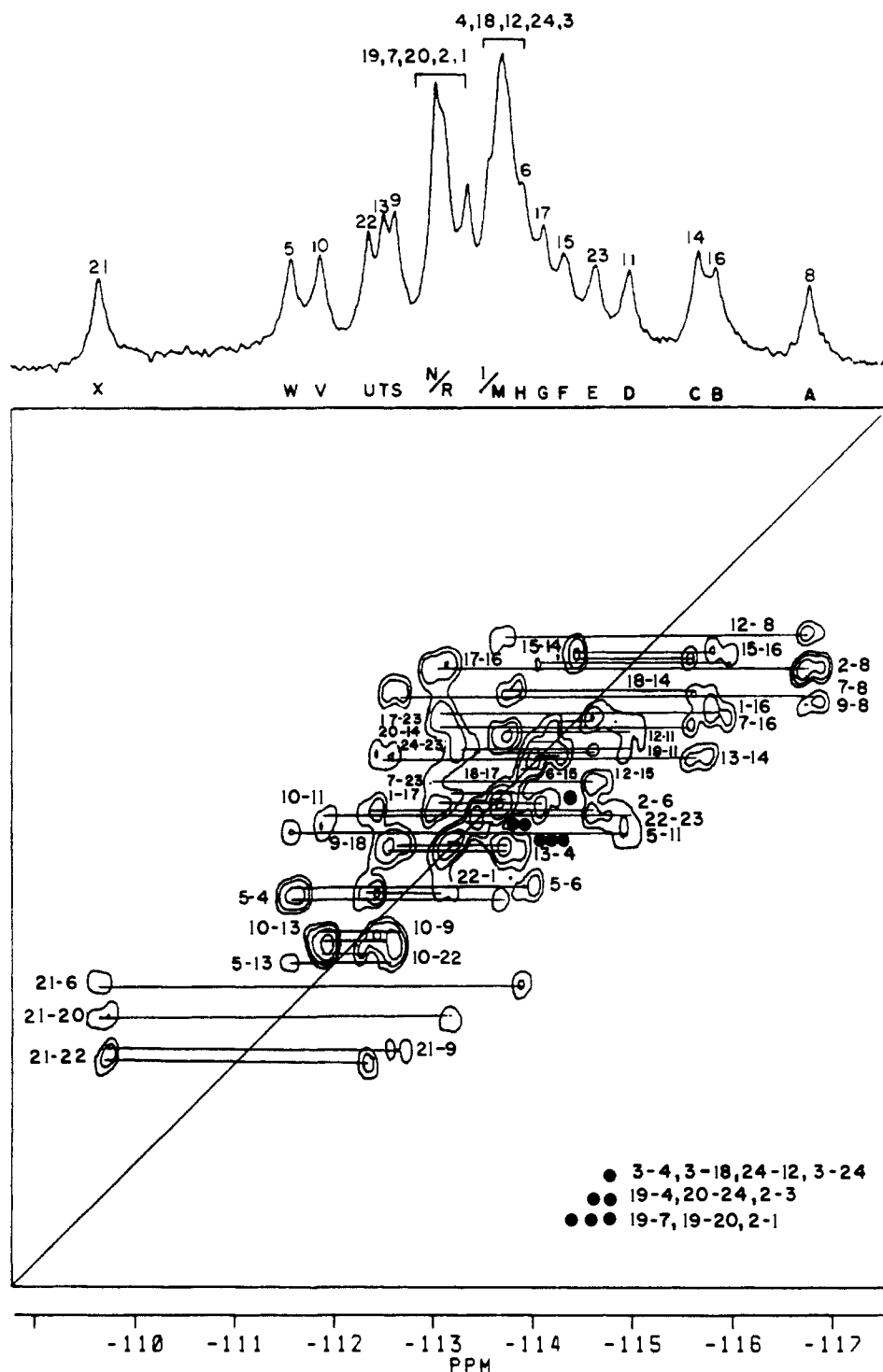


Figure 7. Contour plot of an INADEQUATE experiment on ZSM-5 at 300 K with a 1D MAS NMR spectrum above. 36 experiments with 448 scans in each experiment were carried out with a recycle time of 12 s, and the total time for the experiment was approximately 54 h. A sweep width of 700 Hz, a fixed delay of 15 ms, and 160 real data points were used. Sine-bell and trapezoidal apodizations in F2 and F1 dimensions respectively and a power calculation were used for the data processing.

experiment was therefore emphasized in further work.

Thus, in the INADEQUATE experiment the observed connectivities yield enough information to assign the spectrum. As can be seen from Table II, only four silicon atoms, two in the four-membered rings (Si(9), Si(10)) and two others (Si(7) and Si(12)), have self-connectivities (which will not be detected), and thus they show only three connectivities in the 2D plots. From this, these four signals can be identified as the resonances of F, H, K, and L as indicated by the arrows. The two silicons in the four-membered ring (Si(9), Si(10)) are directly bonded and thus show a connectivity between them, identifying them as resonances K and L. There are two possibilities when starting the assignment from this point where, for example, Si(9) = K or Si(9) = L. Each

of these leads to a complete set of assignments of the resonances, both of which are consistent with the connectivity data as shown in Table II. This is the case for all phases of ZSM-5; it merely reflects the symmetry of the structure, and a decision cannot be made from the present NMR data alone.

Additional information that would help discriminate in favor of one assignment could be gained by combining the NMR data with geometric information from diffraction studies. The differences in chemical shift reflect the differences in the local magnetic environments of the nuclei, and it has been demonstrated previously that correlations exist between average T-T distances and TOT angles and the  $^{29}\text{Si}$  chemical shifts of the resonances for zeolites.<sup>27</sup> Considerable caution must be exercised in the use

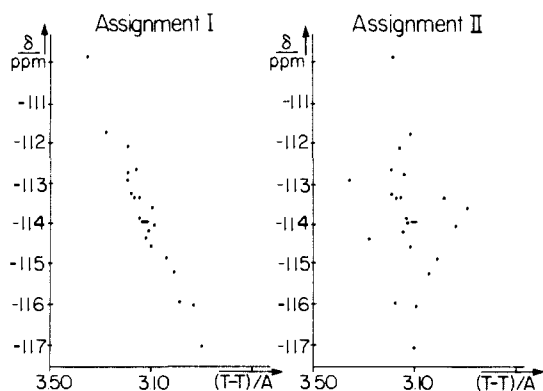


**Figure 8.** Plots of the average T-T distances as functions of the  $^{29}\text{Si}$  chemical shifts for the monoclinic form of ZSM-5. Assignment I corresponds to the numbering of the resonances in Figures 2 and 7 while assignment II is for the alternative numbering where  $T_i \rightarrow T_{i\pm 12}$ .

of correlations of this general type as changes in the average geometric parameters are not large and the errors in the diffraction data are often substantial. However, the use of such correlations here is not to predict the chemical shift of a single resonance but to choose between two possible assignments, which give different patterns. Unfortunately, the present diffraction data<sup>23</sup> are not considered accurate enough to use for this purpose, and the choice of the correct assignment will be left until after discussion of the orthorhombic phase which has been formed from the action of temperature alone.

On increasing the temperature, a phase transition transforms ZSM-5 from the monoclinic phase to the orthorhombic phase (12 T-sites) in the absence of *p*-xylene. Figure 5 shows the results of a 2D INADEQUATE experiment on ZSM-5 at 403 K. The assignment is started at the same point as in the case of the low-loaded form of ZSM-5/*p*-xylene described above. The resonances at lowest fields are assigned as  $T_{10}$  and  $T_9$ . In this spectrum, the overlap of some resonances is more severe and only 18 connectivities out of the 22 are observed, making it more difficult to obtain a complete assignment. In our previous work,<sup>12</sup> smooth and gradual shifts in the various resonances were observed both for the low-loaded ZSM-5 *p*-xylene system on increasing the temperature and for the ZSM-5 spectra at 373 K with increasing concentration of *p*-xylene. Thus some assignments of the resonances of the high-temperature form can be established from the assignments of the low-loaded form of ZSM-5/*p*-xylene discussed above, e.g. the highest field peaks in both cases are both due to the same T-site ( $T_8$  or  $T_{11}$ ). As previously, the signals of  $T_9$  and  $T_{10}$  can be identified as the lowest field resonances. With this information it is now possible to deduce the two sets of assignments completely. For this structure, a high-quality Rietveld analysis of the synchrotron powder X-ray data set is available,<sup>22</sup> and from this, the assignment shown in Figure 2C appears to be the more favorable one. The relation between the two species as discussed above now leads to the choice of the assignment of the low-loaded *p*-xylene form as indicated in Figure 2B. Single-crystal X-ray data on either the high-temperature form or the low-loaded *p*-xylene form should remove any residual ambiguity in these choices.

**II. Monoclinic Phase (24 T-Sites).** It is known from previous work that the monoclinic form of the completely siliceous material exists over a relatively narrow stability field.<sup>12</sup> The present investigation was carried out at 300 K with no *p*-xylene present. Figure 6 shows the results of a 2D COSY experiment on this material and reveals a number of well-defined connectivities. However, as in the case of the orthorhombic form (12 T-sites), many of the interactions are expected to be obscure by the large diagonal peaks. Inspection of Figure 2A shows that most of the spectral intensity in this sample occurs in the center of the

**Table V.** Connectivities of Four-Membered-Ring T-Sites and of the Low-Field Resonances in the Monoclinic Form of ZSM-5

| Known Connectivities from Diffraction Data                     |          |           |           |           |
|--|----------|-----------|-----------|-----------|
| $T_9$  | 8        | <u>10</u> | 18        | <u>21</u> |
| $T_{10}$   | <u>9</u> | 11        | 13        | <u>22</u> |
| $T_{21}$   | 6        | <u>9</u>  | 20        | <u>22</u> |
| $T_{22}$   | 1        | <u>10</u> | <u>21</u> | 23        |
| Observed Connectivities from INADEQUATE Experiments (Figure 7) |          |           |           |           |
| S  | A        | I-M       | <u>V</u>  | <u>X</u>  |
| T  | C        | I-M       | V         | W         |
| U  | E        | N-R       | <u>V</u>  | <u>X</u>  |
| V  | D        | <u>S</u>  | T         | <u>U</u>  |
| W  | D        | H         | I-M       | T         |
| X  | H        | N-R       | <u>S</u>  | <u>U</u>  |

spectrum making the problem much more severe. An INADEQUATE experiment on the same material is presented in Figure 7 and shows many more interactions, 38 of the total 48 expected connectivities (Table III) being observed.

In the orthorhombic form (12 T-sites) the two resonances at lowest field are due to the four silicon atoms in the four-membered rings. On raising the temperature from ambient, there are gradual changes in the frequencies of the different resonances and then a more abrupt change at the transition temperature.<sup>12</sup> In the low-field region, four resonances tend toward the frequencies of the two lowest field signals of the orthorhombic form (12 T-sites). Making specific assignments cannot be absolutely justified because of the discontinuity at the transition temperature, but it was felt that the corresponding resonances in the monoclinic form were probably among those at lower field and particular attention was paid to them in this regard. Table V shows the connectivities of the four silicons in the four-membered ring together with those of the six lowest field resonances in the 1D spectrum. From the underlined connectivities, it can be deduced that silicons 9,22 and 10,21 are the (S,U) and (V,X) pairs, but it is not possible to say which is which.

There are again two possible assignments from this point that are here related by the exchange of  $T_i$  with  $T_{i\pm 12}$ . In order to facilitate discussion, the resonances V and X are assigned to be  $T_{10}$  and  $T_{21}$  at this stage. In Table V the resonances of V and W show the same connectivities to D and T.  $T_{10}$  and  $T_{21}$  are connected to  $T_{11}, T_{13}$  and  $T_6, T_{20}$  respectively besides  $T_9$  and  $T_{22}$ . Table III shows that  $T_5$  is connected to  $T_{11}$  and  $T_{13}$  too, while only  $T_{21}$  is connected to  $T_6$  and  $T_{20}$ . Thus the assignments V to  $T_{10}$ , W to  $T_5$ , and X to  $T_{21}$  can be made, so resonance H corresponds to  $T_6$ . By trial and error, the assignments of D to  $T_{11}$  and T to  $T_{13}$  follow. After this point, the complete assignment can be established. The second possible assignment from the alternative starting point is obtained by exchanging pairs of line assignments as described above.

In this case, combining the NMR and the X-ray data allows a completely unambiguous choice between the two possible assignments. Thus, a highly accurate single-crystal refinement of the room temperature structure has recently been carried out by van Koningsveld and co-workers,<sup>21</sup> and the very low errors in the positional parameters obtained in this study mean that it may reliably be used to distinguish between these two possible assignments. In Figure 8, the average T-T distances are plotted as a functional of chemical shift for both assignments. As can be seen the linear correlation is much better for one of them and this one is considered to be unique. Although both the NMR and diffraction techniques have limitations and are subject to experimental errors, it is thought that their combination leads to an unambiguous answer.

(27) (a) Higgins, J. B.; Woessner, D. E. *EOS* **1982**, *63*, 1139. (b) Smith, J. V.; Blackwell, C. *Nature* **1983**, *303*, 223. (c) Thomas, J. M. et al. *Chem. Phys. Lett.* **1983**, *102*, 158. (d) Groenen, E. J. J. et al. *Zeolites* **1985**, *5*, 361. (e) Engelhardt, G. *Z. Chem.* **1985**, *25*, 252.

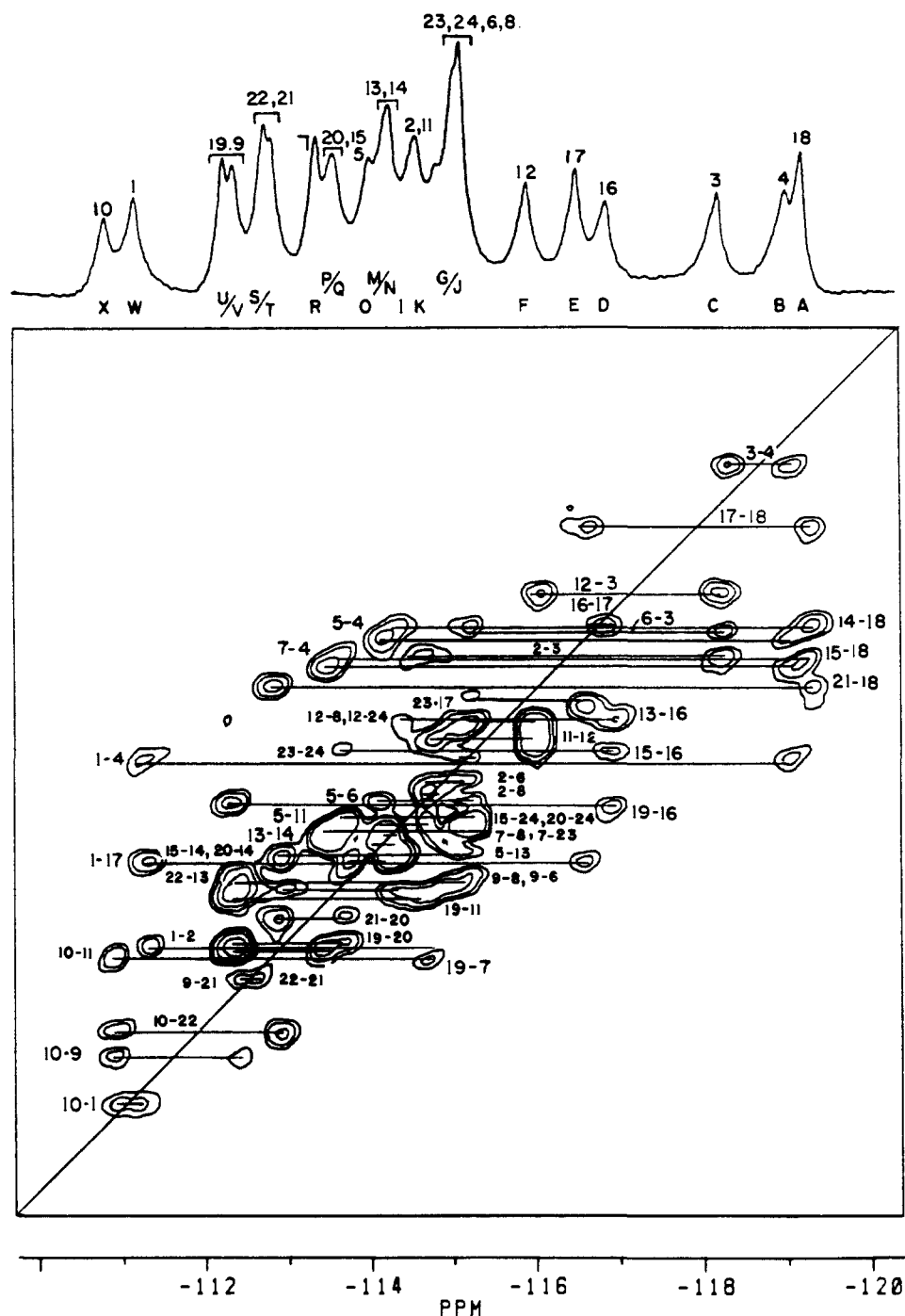


**Figure 9.** Contour plot of a CP-INADEQUATE experiment on ZSM-5 with 8 molecules of *p*-xylene per unit cell with a 1D CP/MAS NMR spectrum on top. 64 experiments with 1088 scans in each experiment were carried out with a recycle time of 3 s, and the total time for the experiment was approximately 58 h. A sweep width of 846 Hz, a contact time of 20 ms, a fixed delay of 16 ms, and 100 real data points were used for the data processing.

**III. Orthorhombic Phase (24 T-Sites).** The results of an INADEQUATE experiment on ZSM-5 loaded with 8 molecules of *p*-xylene per unit cell are shown in Figure 9. In this case 47 of the 48 connectivities are clearly observed. There is nothing known regarding the relationship of the various chemical shifts between this phase and the other phases, but it was thought that the resonances of four silicons in the four-membered ring might well again appear at lower field. Resonance W and the other resonances associated with W (by the 2D plot, Figure 9) are given in Table VI. The first row in this table shows the resonances associated with W, and each column presents the association of the corresponding resonance with the resonances of the first row, respectively. It is shown in Table VI that B and L are simultaneously connected with C. The resonances L and E may or may not be linked to the same resonance (G/J). There are 6 T-sites of the first 12 T-sites that present this kind of connectivity pattern.

**Table VI.** Connectivities Related to Resonance W and T-Site 1

| W   | L | B   | X   | E | 1 | 2 | 4  | 10 | 17 |
|-----|---|-----|-----|---|---|---|----|----|----|
| W   | W | W   | W   |   | 1 | 1 | 1  | 1  |    |
| C   | C | K   | A   |   | 3 | 3 | 9  | 16 |    |
| G/J | O | S/T | D   |   | 6 | 5 | 11 | 18 |    |
| G/J | R | U/V | G/J |   | 8 | 7 | 12 | 23 |    |

(In the case of the orthorhombic phase (24 T-sites) two possible assignments can be made, just as for the monoclinic phase. Thus only the first 12 T-sites are considered.) The resonance W is at lower field and is connected only with one other lower field resonance, X. Thus W could not be the silicon on the four-membered



ring, while X might be among the 6 possible T-sites. Only T<sub>1</sub> is connected with one of the four-membered-ring silicons. The assignment can thus be started at this point, i.e. W = 1 and the assignments X = 10, E = 17, C = 3 and L, B = 2, 4 can now be made. The complete assignment shown in Figure 9 is made by combining the NMR results with diffraction data<sup>28</sup> as described previously. Again, the diffraction experiment was carried out on a single crystal and the positional parameters of the silicon atoms are very accurately defined.

### Conclusions

We have thus demonstrated that 2D <sup>29</sup>Si NMR connectivity experiments may be successfully applied to investigate the three-dimensional bonding in zeolite ZSM-5 in both monoclinic and two orthorhombic forms, the INADEQUATE experiment

(28) van Koningsveld, H.; Tuinstra, F.; van Bekkum, H.; Jansen, J. C. *Acta Crystallogr.* **1989**, *B45*, 423.

being particularly useful. Since ZSM-5 has the most complex unit cell of any known zeolite, with either 12 or 24 inequivalent silicons in the asymmetric unit depending on the form, it should be possible in the future to apply these techniques together with diffraction studies to the determination of unknown zeolite structures. Work of this nature is currently in progress.

**Note Added in Proof.** A single crystal study of the high-temperature structure has recently been completed (van Koningsveld, H.; et al. *Acta Crystallogr. B*, in press). The data are in agreement with the assignment of the resonances of this phase reported in the present work.

**Acknowledgment.** The authors acknowledge the financial assistance of NSERC in the form of Operating and Major Equipment Grants (C.A.F.). G.T.K. acknowledges the Alexander von Humboldt Foundation, C.A.F. the Killam Foundation, and Y.F. the award of a University Graduate Fellowship. They also acknowledge helpful discussions with Prof. H. van Koningsveld.

## Photoinduced Energy Transfer in Multinuclear Transition-Metal Complexes. Reversible and Irreversible Energy Flow between Charge-Transfer and Ligand Field Excited States of Cyanide-Bridged Ruthenium(II)-Chromium(III) and Ruthenium(II)-Rhodium(III) Complexes<sup>1</sup>

Yabin Lei, Tione Buranda, and John F. Endicott\*

Contribution from the Department of Chemistry, Wayne State University, Detroit, Michigan 48202. Received July 20, 1989

**Abstract:** Excited-state relaxation pathways have been examined for some bi- and trinuclear transition-metal complexes containing the Ru(bpy)<sub>2</sub><sup>2+</sup> chromophore linked (or metalated) through cyanide to an ammine chromium(III) or rhodium(III) complex. The (<sup>3</sup>CT)Ru(bpy)<sub>2</sub><sup>2+</sup> absorption and emission maxima and the Ru(III)-(II) reduction potentials all increase in energy with metalation. In most instances energy migration from the initially excited ruthenium center to the acceptor metal centers occurred in discrete steps analogous to elementary chemical reactions between independent molecular species. The migration of energy was manifested by quenching of the (<sup>3</sup>CT)Ru donor emission. This was sometimes accompanied either by (<sup>2</sup>E)Cr(III) phosphorescence emission in the chromium metalates or by the growth of a metal-to-metal charge-transfer absorption in a rhodium metalate. Picosecond flash photolysis has been used to observe the equilibration (in about 1 ns) between the (<sup>3</sup>CT)Ru(bpy)<sub>2</sub><sup>2+</sup> and the triplet ligand field excited states of Rh(NH<sub>3</sub>)<sub>5</sub><sup>3+</sup>. The strongly temperature dependent (<sup>3</sup>CT)Ru(bpy)<sub>2</sub><sup>2+</sup> emission lifetimes of the Rh(NH<sub>3</sub>)<sub>5</sub><sup>3+</sup> metalates are simply described by two competing relaxation channels, one involving unmetalated cyanide (*k*<sub>RuCN</sub>) and the other involving energy transfer to Rh(III) (*k*<sub>Rh</sub>); in principle, one should also allow for a Ru(II)-centered relaxation pathway of the fully metalated complex (*k*<sub>Ru</sub> ≪ *k*<sub>RuCN</sub>), so that τ<sup>-1</sup> = *k*<sub>Ru</sub> + (2-*n*)*k*<sub>RuCN</sub> + *n**k*<sub>Rh</sub> where *n* is the number of metalated cyanides. On the basis of the photophysical behavior (77-298 K) of the parent rhodium hexammine complex, the Ru(bpy)<sub>2</sub><sup>2+</sup> donor is inferred to be strongly coupled to the Rh(NH<sub>3</sub>)<sub>5</sub><sup>3+</sup> and Rh(NH<sub>3</sub>)<sub>4</sub>X<sup>2+</sup> (X = CN, Br, I) acceptor centers but electronically independent unless the donor and acceptor energies become comparable, a situation which may be the case when X = I.

### Introduction

The study of photoinduced electron and energy transfer in simple molecular systems has been a source of conceptual and synthetic chemical challenge to many research groups during the past few years.<sup>2</sup> Much recent work has focused on unresolved

problems in evaluating the factors contributing to the strength of the electronic coupling between donors and acceptors and the relationship between the strength of this coupling and the energy or electron transfer efficiency.<sup>2-23</sup> Covalently linked donor and acceptor systems have been especially useful in some of the more definitive studies.<sup>2,7-10</sup> The strength of the coupling, often ex-

(1) A preliminary account of this work has appeared in the following: Endicott, J. F.; Lessard, R. B.; Lei, Y.; Ryu, C. K. In *Supramolecular Photochemistry*; Balzani, V., Ed.; NATO ASI Series C214; Reidel: Dordrecht, 1987; p 167.

(2) For several pertinent reviews, see: (a) *Supramolecular Photochemistry*; Balzani, V., Ed.; NATO ASI Series C214; Reidel: Dordrecht, 1987. (b) Mikkelsen, K. V.; Ratner, M. A. *Chem. Rev.* **1987**, *87*, 113.

(3) (a) Newton, M. D. *J. Phys. Chem.* **1986**, *90*, 3734. (b) Newton, M. D. *Ibid.* **1988**, *92*, 3049.

(4) Onuchic, J. N.; Beratan, D. N.; Hopfield, J. J. *J. Phys. Chem.* **1986**, *90*, 3707.

(5) Freed, K. F. *J. Chem. Phys.* **1986**, *84*, 2108.

(6) Larsen, S. *J. Chem. Soc., Faraday Trans. 2* **1983**, *73*, 1375.